



Increase of water vapour above the Swiss Plateau from 1995 to 2025 observed by ground-based microwave radiometry

Klemens Hocke^{1,2}, Wenyue Wang³, Leonie Bernet⁴, Alistair Bell^{1,2}, and Christian Mätzler^{1,2}

¹Institute of Applied Physics, University of Bern, 3012 Bern, Switzerland

²Oeschger Centre for Climate Change Research, University of Bern, 3012 Bern, Switzerland

³School of Physical and Chemical Sciences, University of Canterbury, Christchurch, New Zealand

⁴Empa, Swiss Federal Laboratories for Materials Science and Technology, Dübendorf, Switzerland

Correspondence: Klemens Hocke (klemens.hocke@unibe.ch)

Abstract. For climate change research, it is important to have multiple independent measurement techniques. The ground-based microwave radiometer at Bern has been operated since 1994 and allows the independent derivation of the linear trend of the integrated water vapour column or integrated water vapour (IWV). According to the Clausius-Clapeyron equation, the water vapour saturation increases with increase of temperature. There is also a water vapour feedback since water vapour is a natural greenhouse gas and amplifies man-made global warming. In Switzerland, climate change is stronger than at many other places in the world. We analyse observations of the tropospheric water radiometer (TROWARA) which monitored IWV above Bern from 1995 to 2025. The relative IWV increase is 5.1%/decade. Evaluation of coincident IWV data from ERA5 (reanalysis of European Centre for Medium-Range Weather Forecasts) gives a trend of 3.7%/decade. The ERA5 surface air temperature in Bern increased by 0.47K/decade from 1995 to 2025. Thus, we get 10.9% more IWV for a 1K increase in case of TROWARA and 7.8% more IWV for a 1K increase in case of ERA5. Though the IWV trends of TROWARA and ERA5 slightly differ, both datasets agree in the fact that water vapour above the Swiss Plateau significantly increased by 11% or 16% from 1995 to 2025. This strong increase of water vapour certainly has an impact on weather, climate, and hydrology.

1 Introduction

The ERA5 reanalysis data of the 2m air temperature at Bern shows a rate of warming of 0.47K/decade in the time interval from 1995 to 2025. This regional warming trend is larger than the global warming trend which is 0.25K/decade (<https://apps.climate.copernicus.eu/global-temperature-trend-monitor/>). Climate models proved that global warming is caused by the increase of man-made emissions of CO₂ and CH₄ (IPCC, 2013). According to the Clausius-Clapeyron equation, a temperature increase of 1K induces an increase of the saturation water vapour pressure of 7% (Held and Soden, 2006). A higher saturation water vapour pressure means a higher water vapour pressure if the relative humidity remains constant. Bernet et al. (2020) showed that in approximation the integrated water vapour (IWV) is also expected to increase by 7% for a 1K increase of temperature. Water vapour is the strongest natural greenhouse gas and contributes to about 60% of the greenhouse effect for clear skies (Kiehl and Trenberth, 1997). Thus, we can expect that an increase of the water vapour concentration will induce an increase of temperature. The water vapour feedback to a temperature increase is depicted in a scheme in Figure 1.

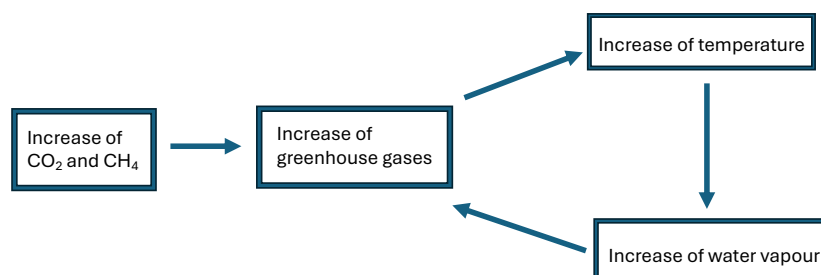


Figure 1. A scheme of the feedback of water vapour to an increase in temperature. Temperature and water vapour will increase until the atmosphere has reached a new equilibrium between evaporation of water and condensation of water vapour.

The loop in Figure 1 should stop when a new equilibrium between evaporation of water and condensation of water vapour is reached. In the worst case, a runaway greenhouse could be generated through the anthropogenic emissions and the water vapour feedback. Climate modeling showed that anthropogenic emissions of greenhouse gases are probably insufficient to generate a runaway greenhouse (Goldblatt et al., 2013).

The monitoring of tropospheric water vapour over several decades with a high accuracy is still a challenge. Radiosonde instruments can change with time, for example, in Switzerland there was a change from Swiss RadioSonde (SRS400) to Sippican in 1999. In recent years, the radiosonde RS41-SG is used in Payerne. The IWV series provided by ERA5 can be affected by such changes in the radiosonde instrumentation. Bernet et al. (2020) found breakpoints in the IWV series measured by receivers of the Global Navigation Satellite System (GNSS). These breakpoints are often associated with exchanges of the GNSS antenna. Ground-based microwave radiometry of IWV series also can have breakpoints as Morland et al. (2009) showed. Because of these uncertainties it is important that IWV trends of multiple instruments are analysed. The trend analysis of Bernet et al. (2020) gave the result that the IWV trends of GNSS, microwave radiometer, Fourier Transform Infrared spectrometer (FTIR) and reanalyses are between 2% and 5%/decade in Switzerland. Global satellite observations in the visible blue spectral range yielded a mean global IWV trend of 2.1%/decade from 2005 to 2020 (Borger et al., 2022). Analyzing the time interval from 1988 to 2014, microwave satellite data of global mean IWV showed a trend of 1%/decade while global mean IWV from ERA5 had a trend of 0.8%/decade (Allan et al., 2022). Combined with a global surface warming trend of 0.17K/decade, the observed trends result into an relative IWV increase of about 6% per 1K in surface air temperature which is close to the expected quotient derived from the Clausius-Clapeyron equation (Allan et al., 2022). Using GNSS station data in Europe from 1994 to 2018, Yuan et al. (2023) found relative IWV trends from about 1.7%/decade in northwest Europe to 5.0%/decade in southeast Europe. The GNSS IWV trends agreed well with the corresponding trends of IWV from ERA5. The



mean value of the European IWV trend differed only by 0.01%/decade in GNSS and ERA5 (Yuan et al., 2023). However, in
45 some European countries ERA5 assimilates the IWV observations of GNSS.

Keihm et al. (2009) reported that the IWV time series of the northern hemisphere (0-60°N, oceanic regions in TOPEX
microwave radiometer data from 1992 to 2005) shows an increase of 2.4%/decade while the southern hemisphere has a smaller
increase of 1.0%/decade. Patel and Kuttippurath (2023) analysed the increase of global tropospheric water vapour in ERA5 data
and found a positive trend of 0.25-1.0 mm/decade. They emphasized that in particular the water vapour in the Arctic strongly
50 increased because of the anomalous rise in temperature in the Arctic. Climate projections indicated that the amount of water
vapour in the Arctic may double at the end of the 21th century (Patel and Kuttippurath, 2023). Viceto et al. (2022) analysed
case studies of poleward transport of water vapour by atmospheric rivers. They argued that atmospheric rivers significantly
contribute to the moistening of the Arctic. Negusini et al. (2021) reported that positive IWV trends dominate at Arctic sites
of GNSS receivers near the borders of the Atlantic Ocean. Sites located at higher latitudes showed no significant values. They
55 emphasized that GNSS measurements of IWV are important in the data sparse regions of the Arctic and Antarctic. Rinke et al.
(2019) derived a positive IWV trend of 0.33 mm/decade in summer in the Arctic region northward of 70°N using 4 global
reanalyses and radiosonde data from 1979 to 20116. They concluded that the Arctic had become wetter overall, but a few
regions show drying.

Ren et al. (2023) compared the water vapour trend results of 4 global reanalysis datasets and found trend values between 0.36
60 to 0.40 mm/decade for the time interval 2000 to 2020. The corresponding relative IWV trend values ranged from 1.96%/decade
to 2.66%/decade. In addition, Ren et al. (2023) calculated a significant positive correlation of 0.68-0.79 between the increase
of IWV and the increase of flood disaster frequency from 1958 to 2020. They argued that rising of IWV has a positive impact
on precipitation changes, increasing the probability of extreme precipitation.

The present study is an update of the trend study by Bernet et al. (2020). It is justified since the observed IWV series at
65 Bern is now 7 years longer than in the past study. The IWV series of the present study comprises in total a time interval of 31
years from 1995 to 2025. There were also two former trend studies with the IWV series of the tropospheric water radiometer
(TROWARA) at Bern. While Morland et al. (2009) obtained a trend of 3.9%/decade for the time interval 1996 to 2007, a trend
study by Hocke et al. (2011) gave no trend at all for the annual means of IWV of the same IWV series but with filled data gaps
and for the time interval 1995 to 2009. In both cases, the time intervals of 12 or 15 years were too short for a reliable IWV
70 trend detection since the large natural interannual variability of IWV can mask the long-term trend of IWV. Contrary to these
early trend studies of TROWARA data, Bernet et al. (2020) found a significant positive trend of 4.8%/decade \pm 1.0%/decade,
where the latter is the 1σ uncertainty, at Bern for the time interval 1995 to 2018. The corresponding ERA5 trend of IWV was
2.3%/decade \pm 0.75%/decade. Hicks-Jalali et al. (2020) reported that IWV increased by 1.3 mm/decade observed by a Raman
lidar at Payerne (close to Bern) from 2009 to 2019. This increase of IWV is consistent with a surface temperature increase of
75 1.38K/decade.

In the following, Section 2 describes the datasets and the data analysis. The results are presented in Section 3. The discussion
of the results is in Section 4, and conclusions are given in Section 5.



2 Datasets and data analysis

2.1 The tropospheric water radiometer TROWARA

80 The microwave radiometer TROWARA has been operated since November 1994 in Bern in the Swiss Plateau (46.95°N, 7.44°E, 575m a.s.l.). The initial setup of TROWARA was described by Peter and Kämpfer (1992). TROWARA measures the thermal microwave emission at the frequencies 21.39, 22.24, and 31.5GHz. The time resolution is about 7 seconds, and the antenna elevation angle is 40°. The voltages of the sky measurement are calibrated by means of noise diodes and matched waveguide terminations which serve as cold and hot loads for TROWARA (Wang et al., 2023). Every half year the internal
85 calibration of TROWARA is controlled and corrected by a tipping curve calibration of the clear sky. The retrieval derives the atmospheric opacities from the observed and calibrated brightness temperatures. The opacities are linearly depending on the retrieval targets IWV and integrated liquid water (ILW) as described by Mätzler and Morland (2009). In addition, it is possible to derive the rain rate as explained and tested in several studies (Wang et al., 2021, 2025a, b).

The retrieved IWV values are most reliable for rain-free periods when ILW is less than 0.4mm (Morland et al., 2009; Hocke
90 et al., 2021). For the time interval 2001 to 2018, the difference of the TROWARA IWV mean and the radiosonde IWV mean was just 0.02mm where the radiosondes were launched in Payerne which is about 40km to the southwest of Bern (Hocke et al., 2021). The present IWV trend analysis is restricted to rain-free periods, similar to the past trend studies for TROWARA (Bernet et al., 2020; Hocke et al., 2011; Morland et al., 2009).

The IWV series before November 2002 has several data gaps due to the fact that TROWARA was operated outdoors. These
95 data gaps were filled by means of IWV data from a nearby indoor microwave radiometer (Hocke et al., 2011). Morland et al. (2009) harmonized the IWV series of TROWARA by means of surface station data of humidity in the vicinity of Bern. The breakpoints in the TROWARA IWV series were mainly due to changes in the radiometer in the time before 2002. It was a good idea to move TROWARA into a indoor laboratory since the TROWARA is very stable after November 2002 when the indoor operation of TROWARA began. After November 2002, the IWV series has almost no data gaps and breakpoints, so that the
100 TROWARA dataset did not require harmonisation procedures after 2002. Wang et al. (2023) described the indoor operation of TROWARA in detail and compared the indoor IWV data to coincident observations of a nearby outdoor radiometer (HATPRO: Humidity and Temperature Profiler). The outdoor radiometer suffered under water films on its radom during and after rain events.

The IWV, ILW, and rain rate data of TROWARA were used in numerous scientific studies. Mätzler et al. (2010) investigated
105 the microwave absorption of supercooled water clouds by using TROWARA and satellite measurements. They compared the observed results to results of various models for the dielectric properties of water. Cossu et al. (2015b) derived and discussed a cloud fraction climatology of liquid water clouds above Bern, while Hocke et al. (2016) analysed the trend of cloud fraction derived from the ILW observations of TROWARA. Cossu et al. (2015a) compared the atmospheric water parameters of TROWARA with coincident data of the Weather Research and Forecasting model WRF. Wang et al. (2022) described atmospheric effects and precursors of rainfall over the Swiss Plateau by using the TROWARA dataset, and Hocke et al. (2019)
110 analysed the diurnal cycle of short-term fluctuations of IWV from TROWARA. Hocke et al. (2017) derived the diurnal cycles



in cloud fraction, ILW, and IWV for different seasons and the annual mean. Wang et al. (2025c) retrieved IWV under clear-sky conditions from the infrared channel data of TROWARA by means of machine learning and by using the microwave data of TROWARA as a training dataset. These examples show that the TROWARA dataset is frequently used and well explored which is of benefit for the present trend study of IWV from TROWARA.

2.2 ERA5

ERA5 is the fifth generation ECMWF reanalysis for the global climate and weather for the past 8 decades (Hersbach et al., 2020). The grid resolution is 0.25° in latitude and longitude. The time series of IWV and 2m air temperature at Bern were interactively generated at Copernicus Climate Change Service (C3S) Climate Data Store (CDS) (<https://cds.climate.copernicus.eu>). Here, we used ERA5 monthly averaged data on single levels from 1940 to present. The model level height at Bern is 706m. Thus, we have to adjust the IWV values of ERA5 from the model height (706m for lowest level at Bern) to the height of TROWARA (575m) by means of an empirical formula (Parracho et al., 2018).

$$\Delta IWV = 4 \times 10^{-4} IWV (h_{model} - h_{TROWARA}) \quad (1)$$

with h in meters. That means, the corrected IWV is equal to IWV plus ΔIWV .

2.3 Radiosonde

In the present study, we use the atmospheric profiles of the radiosondes RS41-SG in 2025 which are launched every day at 11:00 and 23:00 UTC at MeteoSwiss station in Payerne. Since the station is a bit lower in height than Bern, we only use the profile data above 575m (altitude of TROWARA). The RS41-SG provides the dew point temperature. The water vapour pressure is then equal to the saturation vapour pressure of the dew point temperature. We used the formulas for saturation vapour pressure over ice and over liquid as provided by Sonntag (1994). The calculation of IWV from the water vapour pressure profile was described by Hocke et al. (2021).

2.4 GNSS

We use the GNSS IWV data from Payerne for the intercomparison of multiple techniques in the year 2025. The GNSS IWV data at Payerne (491m a.s.l.) is adjusted to Bern (575m a.s.l.) by means of formula 1. The calculation of IWV from the path delay data of the GNSS receiver was described in Hocke et al. (2021).

3 Results

In order to get an impression for the different IWV values of the measurement techniques GNSS (at Payerne), ground-based microwave radiometry (TROWARA at Bern), radiosonde RS41-SG (launched at Payerne) and reanalysis ERA5 (for Bern), Figure 2 shows the intercomparison of the monthly IWV values in 2025.

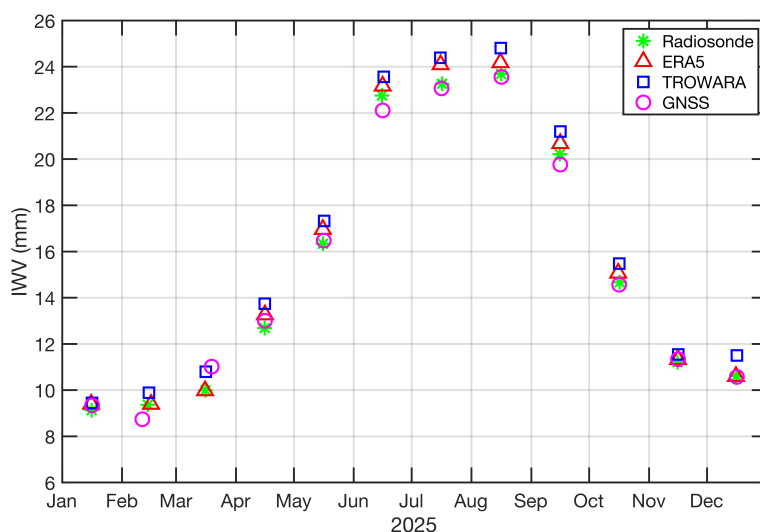


Figure 2. Monthly means of IWV at Bern and Payerne in 2025. Multiple measurement techniques and ERA5 are compared.

140 A good agreement is achieved for all IWV values in the months January and November. In the other months a spread of about 1mm or less is achieved. ERA5 seems to be in the center of the observations, and TROWARA is mostly at the upper boundary. It is difficult to determine the causes of the deviations. One reason is certainly that Bern and Payerne are in a distance of about 40km. The location of the radiosonde observations always vary depending on the wind field, and the radiosonde data are limited to 11:00 and 23:00UTC.

145 Figure 3 shows the time series of monthly means of IWV at Bern from 1995 to 2025 as measured by TROWARA and provided by ERA5. The monthly IWV series of TROWARA and ERA5 have a correlation coefficient of 0.93. The mean difference and the standard deviation of (TROWARA – ERA5) is -0.25 ± 0.42 mm. We calculated the linear trends of the annual means of IWV by means of linear regression. TROWARA has a significant positive IWV trend of 0.08 ± 0.01 mm/y or a relative trend of $5.1\% \pm 0.9\%$ /decade while ERA5 has a significant IWV trend of 0.06 ± 0.01 mm/y or $3.7\% \pm 0.6\%$ /decade.
150 The relative trends are with respect to the mean value of IWV from 1995 to 2025. Figure 3 also shows that the minima and maxima of IWV observed by TROWARA are often lower or higher than those of ERA5.

The time series of the annual means of IWV from TROWARA and ERA5 are shown in Figure 4. From 1994 to 2010, TROWARA had less water vapour than ERA5. Since 2010 the agreement between the absolute annual means of IWV from TROWARA and ERA5 has been improved (for unknown reasons). The higher IWV trend of TROWARA compared to the IWV trend of ERA5 is mainly due to the higher IWV values of ERA5 in the years before 2010. It is hard to determine whether ERA5 or TROWARA were better in the years before 2010. The beginning part of TROWARA's IWV series, where the deviations from ERA5 occur, was carefully harmonized and validated in the trend study of Morland et al. (2009). In 2007, ERA5's IWV is about 1mm larger than TROWARA's IWV. IWV measurements by the GNSS at Payerne suggest that IWV of ERA5 is mostly
155

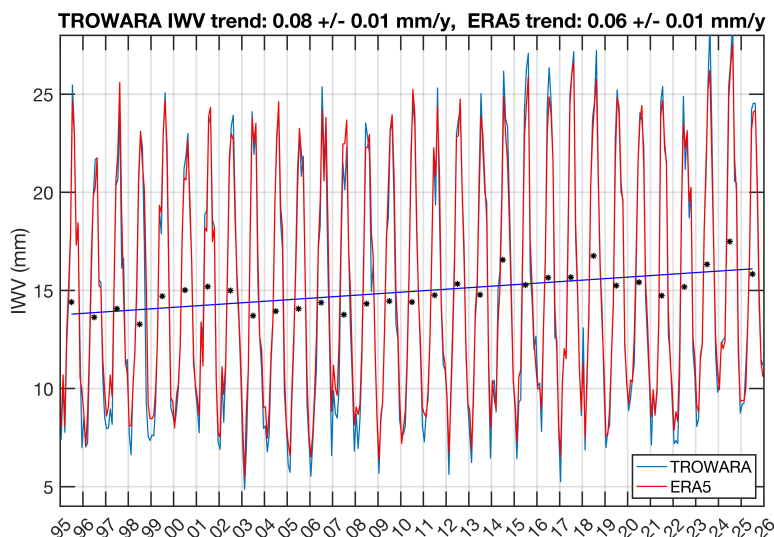


Figure 3. Time series of monthly means of IWV at Bern from 1995 to 2025 provided by TROWARA (blue) and ERA5 (red). In addition, the linear regression line (blue) and the annual means (black) of TROWARA's IWV are shown.

correct, and that TROWARA had a dry bias from January to March 2007. The main result of Figure 4 is that TROWARA and
160 ERA5 show both significant positive IWV trends at Bern.

Figure 5 depicts the seasonal variations of the linear trends of IWV at Bern from 1995 to 2025. The blue curve of TROWARA's monthly IWV trends is slightly larger than those of ERA5 (red curve). Both curves show a similar seasonal variation with a maximal trend in June.

Figure 6 shows the the seasonal trends of IWV (red) and 2m air temperature (blue) from ERA5 at Bern from 1995 to 2025.
165 Both curves are maximal in the summer months from June to September. The linear trend of the annual means of temperature at 2 m is $0.47\text{K} \pm 0.10\text{K}$. Thus, we get an IWV increase of 7.8% per 1K increase in temperature for ERA5. In case of TROWARA, the IWV increase is 10.9% per 1K increase in temperature.

4 Discussion

The trend analysis showed that ground-based microwave radiometry as well as ERA5 reanalysis have significant positive trends
170 of IWV at Bern from 1995 to 2025. Since the past trend study of Bernet et al. (2020) the IWV trend of TROWARA slightly increased from 4.8%/decade to 5.1%/decade, and the IWV trend of ERA5 increased from 2.3%/decade to 3.7%/decade. These increases are mainly due to the high value of IWV at Bern in 2024 (Figure 4). It is remarkable that the interannual variability of IWV strongly increased since 2014 (Figure 4). The interannual variability of IWV seems to be not related to the variability of the North Atlantic Oscillation (NAO) index.

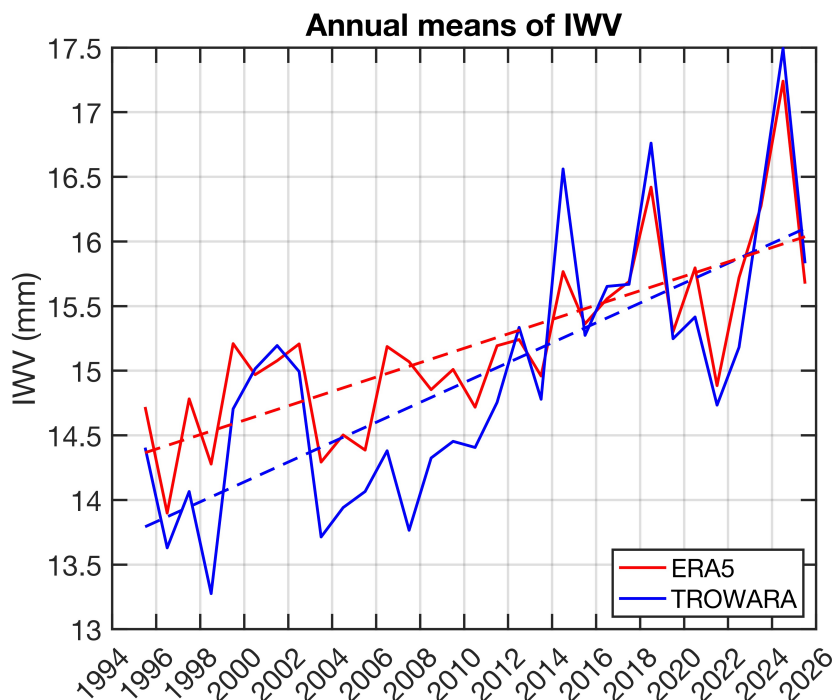


Figure 4. Time series of annual means of IWV for TROWARA and ERA5 at Bern. The dashed lines are the linear regression lines showing the linear IWV trends from 1995 to 2025.

175 The IWV trend values of ERA5 and TROWARA are close to the IWV trends in GNSS time series of southeast Europe in Yuan et al. (2023) who reported a 5%/decade IWV trend for 1994 to 2018. Bernet et al. (2020) analysed the IWV trends of Swiss GNSS stations and found a wide spread from 0.1%/decade (Bern) to 7.0%/decade (Payerne). It is difficult to decide which measurement technique is the best for a reliable detection of IWV trends. Also, the ERA5 reanalysis can have a bias since ERA5's IWV trend significantly depends on the homogeneity of the assimilated humidity profiles from radiosondes. In
180 Switzerland, the radiosonde humidity sensors changed several times during the past three decades. A tiny systematic change in the radiosonde measurement already can increase or decrease the IWV trend value. Figures 3 and 4 also show that TROWARA's IWV was a bit smaller than those of ERA5 in the years before 2010. Particularly, during winter time, TROWARA's IWV minima are lower than those of ERA5. A reason could be wet deposit on the balloon during its ascent through a low stratus layer, and evaporation of the wet deposit when the balloon is above the cloud layer. Low stratus is very common above the
185 Swiss Plateau during winter.

In case of the TROWARA radiometer, the years before 2002 (when the radiometer was operated outdoor) are most critical since several break points and data gaps occurred which were repaired in a great effort by Morland et al. (2009) and Hocke et al. (2011). After 2002, when TROWARA changed into a indoor laboratory, the IWV series of TROWARA had almost no data gaps (less than 2%) and no breakpoints have been noticed. The best agreement between TROWARA and ERA5 is in recent

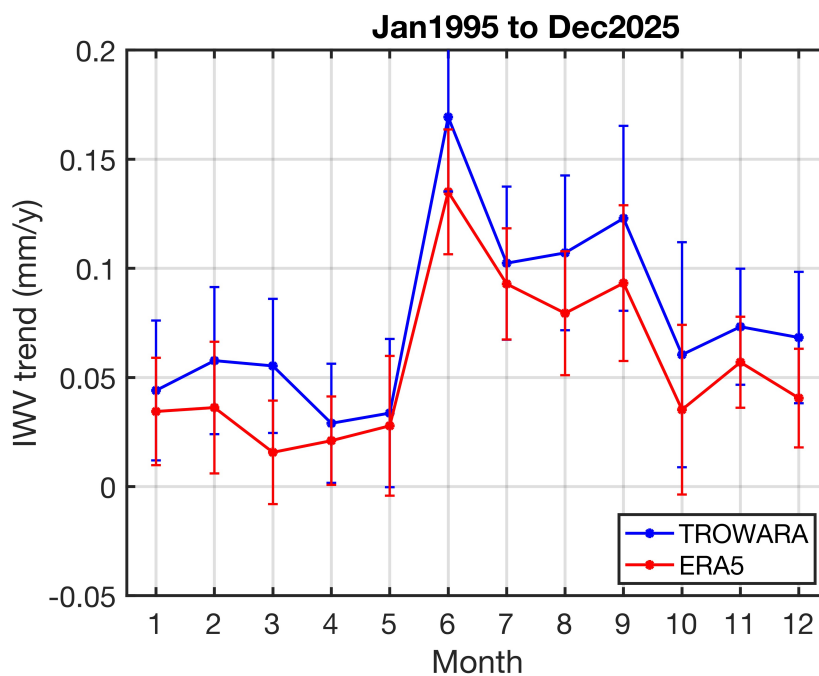


Figure 5. Seasonal IWV trends of TROWARA (blue) and ERA5 (red) at Bern from 1995 to 2025. The IWV trends are maximal in June.

190 years since 2010. This discussion of the advantages and disadvantages of the different IWV datasets shows the importance to
maintain as much independent measurement techniques as possible, so that the IWV trends can be cross-validated (Bernet et al.,
2020). The intercomparison with ERA5 of the present study shows that a ground-based microwave radiometer can provide a
robust IWV series over 31 years, especially if the radiometer is operated indoors (Wang et al., 2023). We are not aware of
a IWV trend study based on data from the commercial outdoor radiometers HATPRO, possibly a wet radom contributes to
195 positive IWV biases.

The positive IWV trends of TROWARA and ERA5 confirm each other and can be explained by the coincident increase of
surface air temperature at Bern from 1995 to 2025. The temperature trend is $0.47\text{K} \pm 0.10\text{K}$. According to Clausius-Clapeyron,
we expect an IWV increase of 7% per 1K increase of temperature. The trend values of TROWARA and ERA5 at Bern indicate
10.9% per 1K increase in temperature for TROWARA and 7.8% per 1K increase in temperature for ERA5. Both values are
200 reasonable.

5 Conclusions

Since the 1990s, climate warming has been quite strong at Bern with a 2m air temperature trend of $0.47\text{K} \pm 0.10\text{K}$ (ERA5
reanalysis 1995 to 2025). The climate in the end of 2025 is about 1.5K warmer than in 1995. Following the Clausius-Clapyron
equation, we would expect that the saturation water vapour pressure increased by about 10.5% from 1995 to 2025 enabling

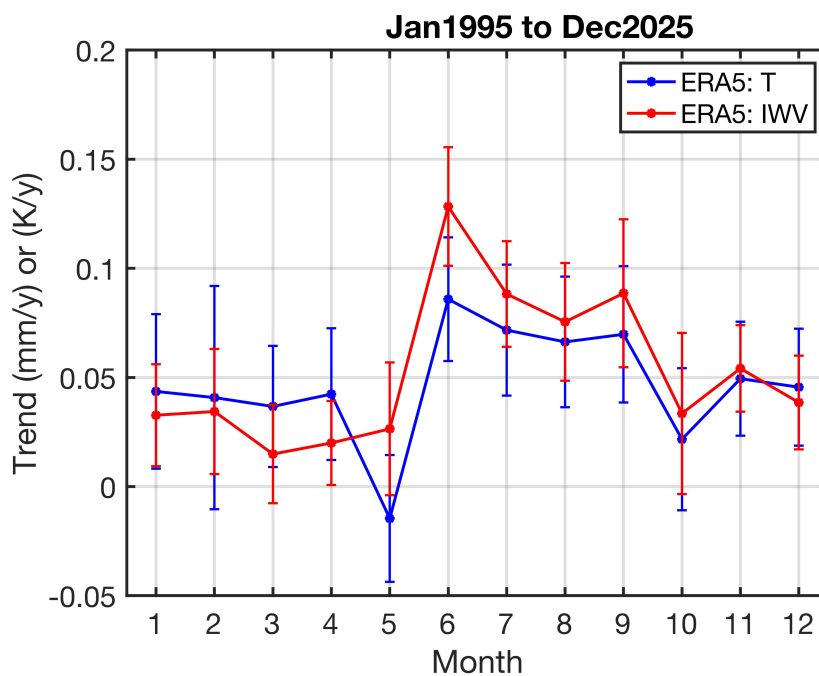


Figure 6. Seasonal trends of IWV (red) and 2m air temperature (blue) from ERA5 at Bern from 1995 to 2025. The seasonal variations are quite similar for both parameters.

205 higher values of water vapour pressure in the air. Bernet et al. (2020) showed that a similar relative increase can be expected for IWV.

The ground-based microwave radiometer TROWARA at Bern measured a relative increase of IWV by 15.8% while the reanalysis ERA5 gave a relative IWV increase by 11.5% from 1995 to 2025. In both cases, one can say that the tropospheric water vapour at the end of 2025 is clearly larger than in 1995 which should have an impact on climate, weather, and hydrology of the Swiss Plateau. The Clausius-Clapeyron equation shows that this water vapour increase is due to climate warming. Linear regression gave a significant positive IWV trend of $5.1\% \pm 0.9\%/decade$ for TROWARA, while ERA5 had a significant IWV trend of $3.7\% \pm 0.6\%/decade$. These values agree well with other IWV trend studies (Yuan et al., 2023; Bernet et al., 2020). The relation between IWV increase and surface air temperature increase is 10.9% IWV increase per 1K increase in temperature in case of TROWARA, and 7.8% IWV increase per 1K increase in temperature in case of ERA5.

215 We cannot exclude that the TROWARA radiometer and ERA5 may have some IWV biases. Particularly in the years before 2010, TROWARA's IWV was smaller than the IWV of ERA5. It is hard to determine possible reasons for this differences in the years before 2010. The main result of the present study remains that both TROWARA and ERA5 have significant positive IWV trends. While ERA5 strongly depends on the assimilated radiosonde measurements, TROWARA is independent of the radiosondes and ERA5 and relies on ground-based microwave radiometry. During the past decades, we had the experience that



220 the indoor operation of the TROWARA microwave radiometer was very valuable for seamless, robust, and accurate monitoring of IWV, demanding only little work craft (Wang et al., 2023).

Data availability. The ERA5 data are available at Copernicus Climate Change Service (C3S) Climate Data Store (CDS) (<https://cds.climate.copernicus.eu> (accessed on 3 February 2026)). Here, we used ERA5 monthly averaged data on single levels from 1940 to present. The monthly IWV series of TROWARA is provided at <https://doi.org/10.48620/94375>.

225 *Author contributions.* K.H. wrote the text. All authors worked on the data analysis, data curation, and operation of TROWARA. All authors checked the manuscript.

Competing interests. The authors declare no conflicts of interest.

Acknowledgements. We thank the engineers for development and taking care of the TROWARA instrument. The reviewers and the editor are thanked for their work.



230 References

- Allan, R. P., Willett, K. M., John, V. O., and Trent, T.: Global Changes in Water Vapor 1979–2020, *Journal of Geophysical Research: Atmospheres*, 127, e2022JD036728, <https://doi.org/https://doi.org/10.1029/2022JD036728>, e2022JD036728 2022JD036728, 2022.
- Bernet, L., Brockmann, E., von Clarmann, T., Kämpfer, N., Mahieu, E., Mätzler, C., Stober, G., and Hocke, K.: Trends of atmospheric water vapour in Switzerland from ground-based radiometry, FTIR and GNSS data, *Atmospheric Chemistry and Physics*, 20, 11 223–11 244, <https://doi.org/10.5194/acp-20-11223-2020>, 2020.
- 235 Borger, C., Beirle, S., and Wagner, T.: Analysis of global trends of total column water vapour from multiple years of OMI observations, *Atmospheric Chemistry and Physics*, 22, 10 603–10 621, <https://doi.org/10.5194/acp-22-10603-2022>, 2022.
- Cossu, F., Hocke, K., Martynov, A., Martius, O., and Mätzler, C.: Atmospheric water parameters measured by a ground-based microwave radiometer and compared with the WRF model, *Atmospheric Science Letters*, 16, 465–472, <https://doi.org/10.1002/asl.583>, 2015a.
- 240 Cossu, F., Hocke, K., and Mätzler, C.: A 10-year cloud fraction climatology of liquid water clouds over Bern observed by a ground-based microwave radiometer, *Remote Sensing*, 7, 7768–7784, <https://doi.org/10.3390/rs70607768>, 2015b.
- Goldblatt, C., Robinson, T. D., Zahnle, K. J., and Crisp, D.: Low simulated radiation limit for runaway greenhouse climates, *Nature Geoscience*, 6, 661–667, <https://doi.org/10.1038/ngeo1892>, 2013.
- Held, I. M. and Soden, B. J.: Robust Responses of the Hydrological Cycle to Global Warming, *Journal of Climate*, 19, 5686 – 5699, <https://doi.org/10.1175/JCLI3990.1>, 2006.
- 245 Hersbach, H., Bell, B., Berrisford, P., Hirahara, S., Horanyi, A., Muñoz-Sabater, J., Nicolas, J., Peubey, C., Radu, R., Schepers, D., Simmons, A., Soci, C., Abdalla, S., Abellan, X., Balsamo, G., Bechtold, P., Biavati, G., Bidlot, J., Bonavita, M., Chiara, G. D., Dahlgren, P., Dee, D., Diamantakis, M., Dragani, R., Flemming, J., Forbes, R., Fuentes, M., Geer, A., Haimberger, L., Healy, S., Hogan, R. J., Holm, E., Janiskova, M., Keeley, S., Laloyaux, P., Lopez, P., Lupu, C., Radnoti, G., de Rosnay, P., Rozum, I., Vamborg, F., Villaume, S., and Thepaut, J. N.: The ERA5 global reanalysis, *Quarterly Journal of the Royal Meteorological Society*, 146, 1999–2049, <https://doi.org/10.1002/QJ.3803>, 2020.
- 250 Hicks-Jalali, S., Sica, R. J., Martucci, G., Maillard Barras, E., Voirin, J., and Haeferle, A.: A Raman lidar tropospheric water vapour climatology and height-resolved trend analysis over Payerne, Switzerland, *Atmospheric Chemistry and Physics*, 20, 9619–9640, <https://doi.org/10.5194/acp-20-9619-2020>, 2020.
- 255 Hocke, K., Kämpfer, N., Gerber, C., and Mätzler, C.: A complete long-term series of integrated water vapour from ground-based microwave radiometers, *International Journal of Remote Sensing*, 32, 751–765, 2011.
- Hocke, K., Navas Guzmán, F., Cossu, F., and Mätzler, C.: Cloud fraction of liquid water clouds above Switzerland over the last 12 years, *Climate*, 4, 48, <https://doi.org/10.3390/cli4040048>, 2016.
- Hocke, K., Navas-Guzmán, F., Moreira, L., Bernet, L., and Mätzler, C.: Oscillations in atmospheric water above Switzerland, *Atmospheric Chemistry and Physics*, 17, 12 121–12 131, <https://doi.org/10.5194/acp-17-12121-2017>, 2017.
- 260 Hocke, K., Liu, H., Pedatella, N., and Ma, G.: Global sounding of F region irregularities by COSMIC during a geomagnetic storm, *Annales Geophysicae*, 37, 235–242, <https://doi.org/10.5194/angeo-37-235-2019>, 2019.
- Hocke, K., Bernet, L., Wang, W., Mätzler, C., Hervo, M., and Haeferle, A.: Integrated Water Vapor during Rain and Rain-Free Conditions above the Swiss Plateau, *Climate*, 9, <https://doi.org/10.3390/cli9070105>, 2021.



- 265 IPCC: Climate Change 2013: The Physical Science Basis. Contribution of Working Group I to the Fifth Assessment Report of the Intergovernmental Panel on Climate Change, Cambridge University Press, Cambridge, United Kingdom and New York, NY, USA, ISBN ISBN 978-1-107-66182-0, <https://doi.org/10.1017/CBO9781107415324>, 2013.
- Keilm, S., Brown, S., Teixeira, J., Desai, S., Lu, W., Fetzer, E., Ruf, C., Huang, X., and Yung, Y.: Ocean water vapor and cloud liquid water trends from 1992 to 2005 TOPEX Microwave Radiometer data, *Journal of Geophysical Research: Atmospheres*, 114, <https://doi.org/https://doi.org/10.1029/2009JD012145>, 2009.
- 270 Kiehl, J. T. and Trenberth, K. E.: Earth's annual global mean energy budget, *Bulletin of the American Meteorological Society*, 78, 197 – 208, [https://doi.org/10.1175/1520-0477\(1997\)078<0197:EAGMEB>2.0.CO;2](https://doi.org/10.1175/1520-0477(1997)078<0197:EAGMEB>2.0.CO;2), 1997.
- Mätzler, C. and Morland, J.: Refined physical retrieval of integrated water vapor and cloud liquid for microwave radiometer data, *IEEE Transactions on Geoscience and Remote Sensing*, 47, 1585–1594, <https://doi.org/10.1109/TGRS.2008.2006984>, 2009.
- 275 Mätzler, C., Rosenkranz, P. W., and Cermak, J.: Microwave absorption of supercooled clouds and implications for the dielectric properties of water, *Journal of Geophysical Research: Atmospheres*, 115, <https://doi.org/10.1029/2010JD014283>, 2010.
- Morland, J., Collaud Coen, M., Hocke, K., Jeannot, P., and Mätzler, C.: Tropospheric water vapour above Switzerland over the last 12 years, *Atmospheric Chemistry and Physics*, 9, 5975–5988, <https://doi.org/10.5194/acp-9-5975-2009>, 2009.
- Negusini, M., Petkov, B. H., Tornatore, V., Barindelli, S., Martelli, L., Sarti, P., and Tomasi, C.: Water Vapour Assessment Using GNSS and Radiosondes over Polar Regions and Estimation of Climatological Trends from Long-Term Time Series Analysis, *Remote Sensing*, 13, <https://doi.org/10.3390/rs13234871>, 2021.
- 280 Parracho, A. C., Bock, O., and Bastin, S.: Global IWV trends and variability in atmospheric reanalyses and GPS observations, *Atmospheric Chemistry and Physics*, 18, 16 213–16 237, <https://doi.org/10.5194/acp-18-16213-2018>, 2018.
- Patel, V. K. and Kuttippurath, J.: Increase in Tropospheric Water Vapor Amplifies Global Warming and Climate Change, *Ocean-Land-Atmosphere Research*, 2, 0015, <https://doi.org/10.34133/olar.0015>, 2023.
- 285 Peter, R. and Kämpfer, N.: Radiometric determination of water vapor and liquid water and its validation with other techniques, *Journal of Geophysical Research: Atmospheres*, 97, 18 173–18 183, <https://doi.org/https://doi.org/10.1029/92JD01717>, 1992.
- Ren, D., Wang, Y., Wang, G., and Liu, L.: Rising trends of global precipitable water vapor and its correlation with flood frequency, *Geodesy and Geodynamics*, 14, 355–367, <https://doi.org/https://doi.org/10.1016/j.geog.2022.12.001>, 2023.
- 290 Rinke, A., Segger, B., Crewell, S., Maturilli, M., Naakka, T., Nygård, T., Vihma, T., Alshawaf, F., Dick, G., Wickert, J., and Keller, J.: Trends of Vertically Integrated Water Vapor over the Arctic during 1979–2016: Consistent Moistening All Over?, *Journal of Climate*, 32, 6097 – 6116, <https://doi.org/10.1175/JCLI-D-19-0092.1>, 2019.
- Sonntag, D.: Advancements in the field of hygrometry, *Meteorologische Zeitschrift*, 3, 51–66, <https://doi.org/10.1127/metz/3/1994/51>, 1994.
- Viceto, C., Gorodetskaya, I. V., Rinke, A., Maturilli, M., Rocha, A., and Crewell, S.: Atmospheric rivers and associated precipitation patterns during the ACLOUD and PASCAL campaigns near Svalbard (May–June 2017): case studies using observations, reanalyses, and a regional climate model, *Atmospheric Chemistry and Physics*, 22, 441–463, <https://doi.org/10.5194/acp-22-441-2022>, 2022.
- 295 Wang, J., Yi, W., Wu, J., Chen, T., Xue, X., Zeng, J., Vincent, R. A., Reid, I. M., Batista, P. P., Buriti, R. A., Tsuda, T., Mitchell, N. J., and Dou, X.: Coordinated Observations of Migrating Tides by Multiple Meteor Radars in the Equatorial Mesosphere and Lower Thermosphere, *Journal of Geophysical Research: Space Physics*, 127, e2022JA030 678, <https://doi.org/10.1029/2022JA030678>, e2022JA030678
- 300 2022JA030678, 2022.
- Wang, W., Hocke, K., and Mätzler, C.: Physical retrieval of rain rate from ground-based microwave radiometry, *Remote Sensing*, 13, <https://doi.org/10.3390/rs13112217>, 2021.



- Wang, W., Murk, A., Sauvageat, E., Fan, W., Dätwyler, C., Hervo, M., Haefele, A., and Hocke, K.: An Indoor Microwave Radiometer for Measurement of Tropospheric Water, *IEEE Transactions on Geoscience and Remote Sensing*, 61, 1–13, 305 <https://doi.org/10.1109/TGRS.2023.3261067>, 2023.
- Wang, W., Fan, W., and Hocke, K.: Precipitation retrievals for ground-based microwave radiometer using physics-informed machine learning methods, *Journal of Hydrology*, 655, 132 901, <https://doi.org/10.1016/j.jhydrol.2025.132901>, 2025a.
- Wang, W., Fan, W., and Hocke, K.: Rain detection for rain-contaminated ground-based microwave radiometer data using physics-informed machine learning method, *Journal of Hydrology*, 648, 132 365, <https://doi.org/10.1016/j.jhydrol.2024.132365>, 2025b.
- 310 Wang, W., Porcile, C. M., Fan, W., and Hocke, K.: Integrated Water Vapor Estimation During Clear Skies Using a Ground-Based Infrared Radiometer and the Light Gradient Boosting Machine Method, *IEEE Journal of Selected Topics in Applied Earth Observations and Remote Sensing*, 18, 10 724–10 732, <https://doi.org/10.1109/JSTARS.2025.3558761>, 2025c.
- Yuan, P., Van Malderen, R., Yin, X., Vogelmann, H., Jiang, W., Awange, J., Heck, B., and Kutterer, H.: Characterisations of Europe’s integrated water vapour and assessments of atmospheric reanalyses using more than 2 decades of ground-based GPS, *Atmospheric Chemistry and Physics*, 23, 3517–3541, <https://doi.org/10.5194/acp-23-3517-2023>, 2023. 315